Enhancing low-wavenumber information in RWI using energy norm Born scattering

Guanchao Wang (China University of Petroleum-Beijing), Tariq Alkhalifah (King Abdulla University of Science and Technology), Shangxu Wang (China University of Petroleum-Beijing).

Summary

Full waveform inversion (FWI) plays a central role in the field of exploration geophysics due to its potential in recovering the properties of subsurface at a high resolution. A starting model with ample long-wavelength components is essential for the success of most FWI algorithms. Reflection waveform inversion (RWI) is one popular way to invert for the long-wavelength velocity components from the short offset seismic data by decomposing the gradient of FWI into migration and tomographic terms. However, the transmitted part of Born scattering in conventional RWI still produces high-wavenumber artifacts, which would hinder its convergence. Thus, an efficient non-transmission energy norm born scattering is used in RWI to overcome the drawbacks of conventional RWI. We use numerical examples to show that the energy norm born scattering can provide clean transmission energy from the reflector and enhance the low-wavenumber information in the RWI gradient.

Introduction

It has been well-known that both low-wavenumber (reflection and refraction/transmission kernels) and high-wavenumber (migration kernel) components reside in the gradient of conventional FWI. The transmission energy contains sufficient low-wavenumber information and can well illuminate a target region, but it only contributes to the recovery of the shallow part unless the seismic data holds quite long offsets with rich refraction and diving waves. The migration kernel, on the other hand, can update the deep part of the model but it mainly holds high-wavenumber components. Conversely, the reflection kernel inverts for the low-wavenumber of deep part but has generally a weak energy compared to the high-wavenumber migration term, which causes the conventional FWI process to fall into a local minimum.

A slew of strategies has been developed to promote the low-wavenumber components update for the deep part. Xu et al. (2012) first proposed the notion of reflection full waveform inversion with the help of migration and de-migration to update the low-wavenumber along the wave path. To avoid the need for a least square reverse time migration in RWI, several studies adopt the cross-correlation based objective function into the RWI (Ma and Hale, 2013; Chi et al., 2015). Further using the RWI machinery, Alkhailfah and Wu (2016) obtained additional low-wavenumber components from the multi-scattering energy wavepath in the frequency domain. In addition, reflection FWI was extended by Wang et al., (2017，2018), Guo and Alkhalifah (2017) to elastic media.

The aforementioned RWI strategy can improve the reflection kernel, however, the gradient of RWI often still includes high wavenumbers generated from the cross-correlation of the down-going background wavefield and the transmission part of Born scattered wavefield. To attenuate the unwanted high-wavenumber artifacts, we can separate up- and down-going wavefields in the Born scattering (Liu et al., 2011) or precondition the gradient by using a scattering angle-based filter (Alkhalifah, 2015). These approaches, however, impose additional cost to the inversion.

In this abstract, we use the energy norm Born scattering (Sun and Alkhalifah, 2017) in the frequency domain RWI instead of the conventional Born scattering. The energy norm Born scattering can isolate the scattered component from the Born wavefield easily and produce a gradient free of high-wavenumber artifacts. We further update both the background velocity and the short wavelength velocity perturbation simultaneously, and use the inverted velocity perturbation as the source of scattering in the RWI process as opposed to a full frequency band least square migration image, which requires a lot of computation.

We first give a brief introduction of the energy norm Born scattering with a single interface model example. Next, the detailed RWI workflow based on the energy norm Born scattering is followed. At the end, a modified Marmousi model test demonstrates the effectiveness of the proposed algorithm.

Theory

We will first establish the concept of the energy Norm Born scattering, and its main advantage over regular Born. Then, we will incorporate it into reflection full waveform inversion (RWI).

1. Non-transmission Energy Norm Born Scattering

Actually, the pure reflective energy norm Born scattering is the adjoint of the inverse scattering imaging condition (Whitmore and Crawley,2012) or named as energy norm imaging condition (Rocha et al.,2016). The energy norm imaging condition can be stated in frequency domain as,

$$I_E = \sum_\omega \frac{\omega^2}{v^2} u_s(\boldsymbol{x})u_r(\boldsymbol{x}) + \nabla u_s(\boldsymbol{x}) \cdot \nabla u_r(\boldsymbol{x}) \qquad (1)$$

where $u_s(\boldsymbol{x})$ and $u_r(\boldsymbol{x})$ are the source and receiver wavefield in frequency domain, respectively, v is the velocity at the image point $\boldsymbol{x}$, and ∇ is the space gradient operator. In the 2D case, $\nabla = (\frac{\partial}{\partial x}, \frac{\partial}{\partial z})$. We can rewrite equation 1 in compact,

$$I_E = \sum_\omega \boxdot u_s(\boldsymbol{x}) \cdot \boxdot u_r(\boldsymbol{x}) \qquad (2)$$

where the energy operator $\boxdot\, u_s = (\frac{i\omega}{v},\frac{\partial}{\partial x},\frac{\partial}{\partial z})u_s$ acting on the source wavefield, and $\boxdot\, u_r = (\frac{-i\omega}{v},\frac{\partial}{\partial x},\frac{\partial}{\partial z})u_r$ acting on the receiver. Using this concise energy operator, we can easily express the adjoint of equations 1 and 2, regarded as energy norm Born scattering (Sun and Alkhalifah, 2017),

$$d_m = G(x_r, x, \omega)\,\boxdot^T\boxdot\, u_s I_E, \qquad (3)$$

where $G(x_r, x, \omega)$ is the Green's function from space location x to receiver location x_r. The virtual source scattering term of the demigrated data, d_m, can be further derived as,

$$\boxdot^T\boxdot\, u_s I_E = I_E \frac{\omega^2}{v^2} u_s(x) + \nabla \cdot [I_E \nabla u_s(x)]$$
$$= \nabla I_E \cdot \nabla u_s(x) \qquad (4)$$

We highlight the main feature of the energy norm Born scattering with a single interface model. Figure 1 shows the wavefields for the conventional Born scattering (Figure 1a) and the energy norm Born scattering given in equation 3 (Figure 1b). Figure 1 verifies that the properties of this type energy norm Born scattering would attenuate the transmission. To highlight the importance of this feature for RWI, we calculate the corresponding reflection kernels. Figures 2a,2b and 2c,2d show such kernels computed using the conventional and energy norm Born scattering, respectively. We see that the migration ellipse artifacts in RWI, which comes from the cross-correlation of transmission and reflection components, is well attenuated in the application of energy norm Born scattering. The low-wavenumber reflection kernels are free of high vertical wavenumber components, which is expected to lead such to faster convergence in the inversion. There is another type of energy norm Born scattering, which is associated with the non-reflection wave equation. Readers can find details of it in Sun and Alkhalifah (2017), in this abstract we focus on the purely reflection one.
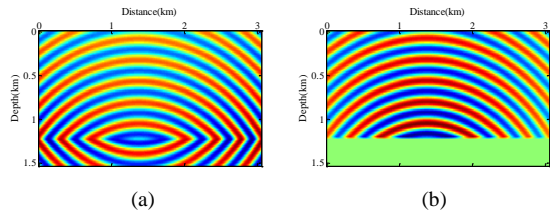

Figure 1: The frquency domain Born scattered wavefield for a single interface model. (a) The conventional Born scattering operator; (b)the energy norm Born scattering operator.
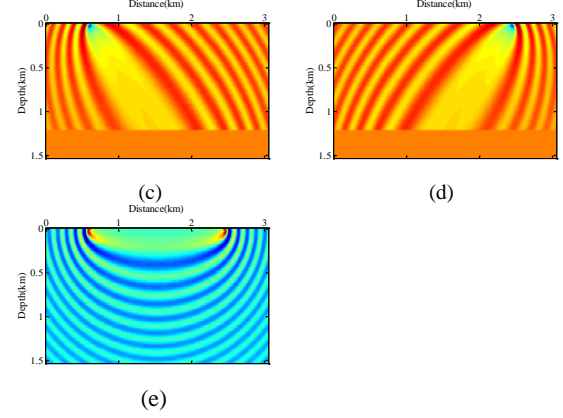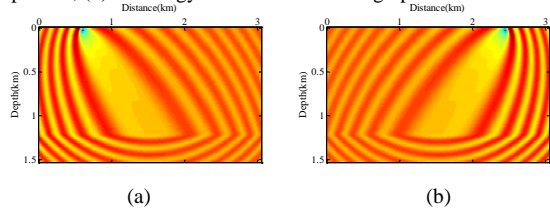

Figure 2: The source and receiver side transmission kernels for conventional born scattering (a and b, respectively), and for the energy norm Born scattering (c and d, respectively). e) the conventional FWI kernel.

2. Review of Reflection Waveform Inversion

Figure 2e shows the conventional FWI kernel, which includes the low-wavenumber wavepath from the source to the receiver. This transmission component can be seen in the RWI kernel (the combination of Figures 2c and 2d), reflecting from the interface. It means this transmission kernel in Figure 2e can update the low-wavenumber as well but limited to a shallow area unless with large offset data. To utilize both low-wavenumber components (FWI and RWI), we use the following misfit function proposed by Alkhalifah and Wu (2016),

$$E(v, \delta v) = \frac{1}{2}\sum_{s,r,\omega}\|d_{syn} + d_m - d_{obs}\|^2 \qquad (5)$$

To obtain a full frequency band image I_E requires a large computational costed, thus in this study the velocity perturbation was used for the demigration process (Equation 4). In equation (5), d_{obs} is the observed data, d_{syn} and d_m are the simulated data using the background velocity v and Born simulated data using the velocity perturbation, δv, respectively.

The background and perturbed velocities are updated simultaneously by minimizing the objective function 5. We deduce the gradient of the functional with respect to velocity perturbation using the adjoint state method (Plessix,2006),

$$\nabla E_{\delta v} = -\frac{2}{v^3}\sum_{s,r,\omega}[\omega^2 u_0(x,\omega) * u^*(x,\omega)] \qquad (6)$$

and the gradient of the background velocity,

$$\nabla E_v = -\frac{2}{v^3}\sum_{s,r,\omega}\omega^2[u_0(x,\omega) * u^*(x,\omega) + \delta u_0(x,\omega) *$$
$$u^*(x,\omega) + u_0(x,\omega) * \delta u^*(x,\omega)] \qquad (7)$$

where u_0 and u^* represent the forward and backward adjoint background wavefields, respectively. The δu_0 and δu^* are the receiver- and source-side energy norm Born scattering wavefields taking the velocity perturbation as the source term.

RWI with energy norm Born scattering

An accurate velocity perturbation image is needed for a stable update of background velocities. Therefore, we optimize the δv for each frequency by fitting it to the residuals. Since the background model is stationary, such optimizations in the frequency domain are cheap, requiring one Stiffness matrix inversion. The background part v is updated using the RWI kernel. The detailed workflow of our suggested energy norm Born scattering RWI is given in Table 1.

Tabe1. RWI workflow with energy norm Born scattering

Inputs: *The recorded data d_{obs} and the initial velocity v*
Outer Loop:
Inner Loop1:
Perform least square algorithm with v to updateδv
Calculate the gradient with respect to δv using equation 6
Update the short wavelength model δv
If Converge End Inner Loop 1
Inner Loop2:
Perform the RWI with δv to update v
Apply energy Born scattering to obtain $\boldsymbol{\delta u_0}, \boldsymbol{\delta u^*}, d_m$
Calculate the gradient with respect to v using equation 7
Update the long wavelength model v
If Converge End Inner Loop 2
If Converge End Outer Loop

Example

We evaluate the effectiveness of the proposed energy norm Born scattering RWI method on the modified Marmousi model, which is shown in Figure3. The Marmousi model here has a size of $nx * nz = 465 * 148$ with a grid interval of 20m in both the horizontal and vertical directions. 45 shots are positioned on the surface at a 200m interval. The wavefields are recorded by 465 receivers covering the entire model at the surface.

Three frequencies (3Hz 3.5Hz and 4Hz) were used in this experiment to demonstrate its effectiveness with limited data. The initial model shown in Figure 4a for this numerical experiment is linearly increasing, 1.5 km/s at the top and 4.0 km/s at the bottom. We first optimize the velocity perturbation by migrating the data $(d_{syn} - d_{obs})$ under the frame of a least square reverse migration using the initial velocity. However, with an inaccurate background velocity model v, the migrated perturbation image shown in Figure 4b is generally inaccurate. The inverted background velocity with the energy norm Born scattering is shown in Figure5a, and the optimal velocity perturbation is shown in Figure 5b. Obviously, the image in Figure5b is considerably better than Figure 4b in positioning the perturbations. For comparison, Figure 7a displays the conventional Born scattering RWI result starting from the linearly increasing initial model. The long-wavelength information was somewhat updated in

Figure 7a, but the high wavenumber components (Black arrow) were also inverted despite the smoothing filter for the RWI gradient.

To verify the long-wavelength velocity was properly inverted by our proposed RWI, the conventional FWI was followed by using the RWI results as initial. Figure 6 is the is the final FWI result using Figure 5a as the starting velocity. Since the starting model free of high-wavenumber artifacts, the inverted velocity is very close to the true model. Figure 7b is the FWI result from Figure 7a. In Figure 7b, some velocity structures are mis-located and the velocity value is not correctly inverted as well due to artifacts in the initial model (Figure7a). As we can conclude from these results, our energy norm Born scattering RWI approach can provide a better starting model for conventional FWI to avoid cycle skipping even in the absence of the low frequencies below 3 Hz.
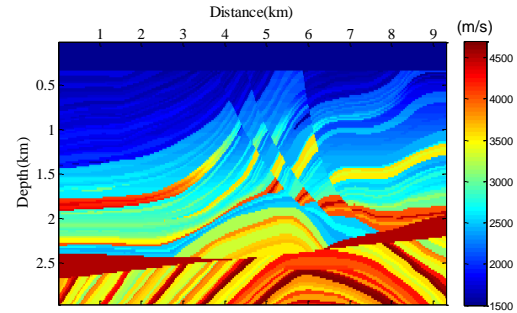

Figure 3: The true modified Marmousi model.

Conclusions

We developed a frequency domain energy norm Born scattering RWI algorithm to remove the high-wavenumber artifacts in the conventional RWI gradient and enhance the long-wavelength velocity updating. The energy norm Born scattering formula can attenuate the transmission and produce pure reflection wavefield to compute the gradient of RWI. The inclusion of energy Born scattering helps mitigate the high-wavenumber artifacts from our RWI results. A numerical test on the Marmousi model demonstrates that our proposed RWI can better invert the long-wavelength velocity, which enable the conventional FWI to converge to a more accurate final result with less iterations
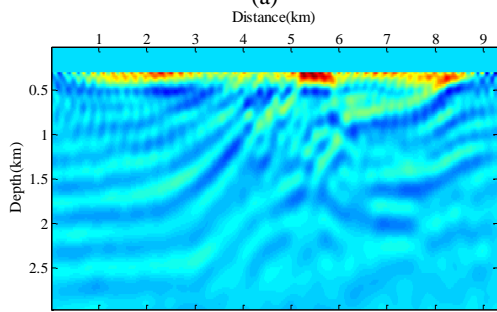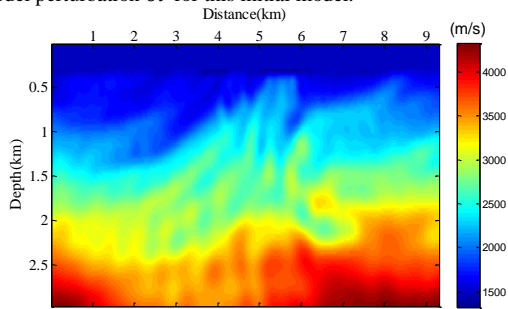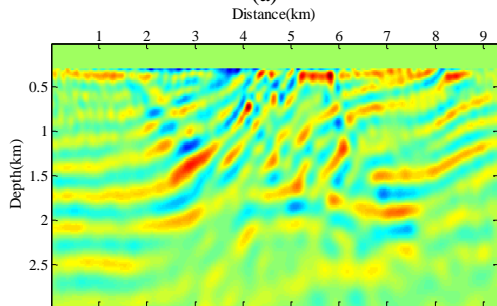
RWI with energy norm Born scattering
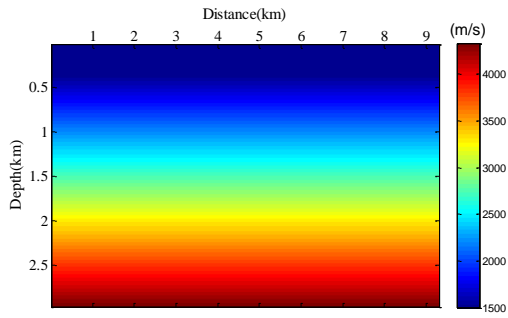
(a)

(b)

Figure 4: (a) The linearly increasing starting model, (b) The inverted model perturbation δv for this initial model.

(a)

(b)

Figure5: (a) The inverted background model v using the energy norm Born scattering based RWI, (b) the inverted model perturbation δv for the (a).
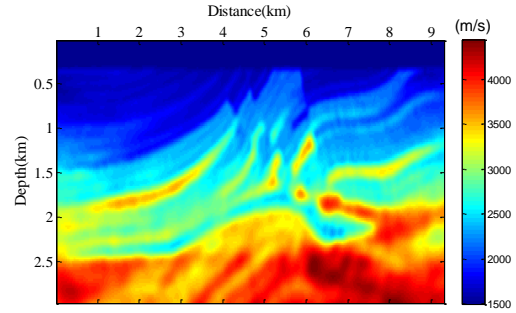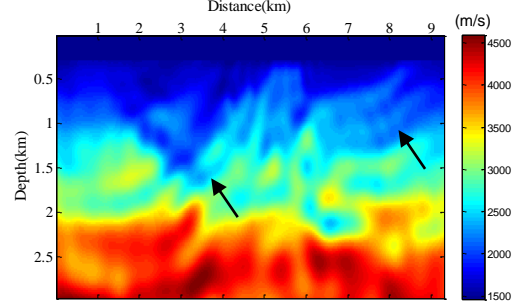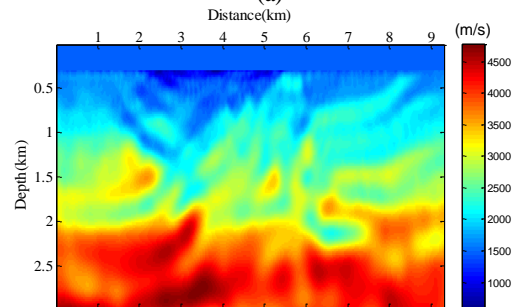

Figure 6: The FWI result from the background model (Figure 5a) with the inverted perturbation (Figure 5b) added to it.

(a)

(b)

Figure 7: (a) The inverted background model v using the conventional Born scattering based RWI, (b) the final FWI result from the background model in (a).